Modeling and Simulation of Trapped-ion Quantum Repeaters and Networks

Charu Jain[*], Chuen Hei Chan[*+], Ezra Kissel[*], Wenji Wu[*], Inder Monga[*]
[*]Lawrence Berkeley National Laboratory, [+]Virginia Tech, USA

Abstract

This paper explores the design and implementation of trapped-ion quantum repeaters and networks using modeling and simulation. We aim to quantitatively understand the practical architecture design and resource requirements of trapped-ion entanglement-based quantum repeater paradigms. Our simulation results explore entanglement rate and fidelity as key performance metrics, and we discuss the major challenges for practical deployment of quantum networks and future directions for research and development in order to meet these challenges.

CCS Concepts

• **Networks** → **Network protocols**; **Network architectures**; **Network components**; **Network performance evaluation**.

Keywords

Quantum repeaters, Quantum networks, Quantum network architecture, Modeling and simulation, Network performance analysis

ACM Reference Format:
Charu Jain[*], Chuen Hei Chan[*+], Ezra Kissel[*], Wenji Wu[*], Inder Monga[*], [*]Lawrence Berkeley National Laboratory, [+]Virginia Tech, USA, . 2025. Modeling and Simulation of Trapped-ion Quantum Repeaters and Networks. In *Quantum Networks and Distributed Quantum Computing (QuNet '25), September 8–11, 2025, Coimbra, Portugal.* ACM, New York, NY, USA, 7 pages. https://doi.org/10.1145/3749096.3750024

1 Introduction

Quantum networks promise to revolutionize how we process and transmit information, potentially enabling unprecedented capabilities in secure communication, distributed computing, and sensing applications. To realize these great potentials, quantum networks are being actively researched and developed worldwide across different physical platforms, from solid-state systems such as superconducting circuits [1], and nitrogen vacancy centers in diamond [2, 3], to neutral atoms [4, 5], and trapped ions [6–9].

Trapped ions are one of the leading platforms for large scale quantum networks due to their unique features. First, they have excellent quantum information processing capabilities. Trapped ions provide inherently identical qubits with long coherence times, which can be initialized, manipulated, entangled, and read out with high fidelity. Trapped ions have demonstrated single-qubit gates of high precision with fidelities of ≥99.995% [10] and two-qubit gates with fidelities near 99.9% for laser-driven gates [10, 11]. Ion qubit state preparation and measurement fidelities ≥99% can be easily achieved [12, 13]. Second, entanglement is the fundamental ingredient for quantum networks, and trapped-ion platforms have inherent support for entanglement generation, distribution, and storage. Trapped ions are ideal single photon emitters that can be entangled with emitted photons. The emitted photons from different ion qubits are transmitted to perform Bell State Measurement (BSM) in order to establish entanglement between remote ion qubits. The established entanglement is finally stored in trapped-ion qubits with long coherence times.

Several building blocks for quantum networking have been developed and demonstrated, in particular, integrating ion traps with optical cavities provides the potential of an on-demand and coherent light-matter interface for quantum networking [14, 15]. High-fidelity quantum frequency conversion converts photons from trapped ions to the optimal telecom wavelengths for long-distance quantum networking [8]. A recent milestone experiment in quantum networks demonstrated the generation of entanglement between two nodes separated by 50 km mediated through an intermediate quantum repeater (QR) based on trapped $^{40}Ca^{+}$ ions [9]. All these works have shown the possibility of generating high-rate and high-fidelity remote entanglement between trapped ions over long distances.

Ideally, quantum network research should be carried out in real network environments. However, this approach has a few constraints. First, building quantum network testbeds is expensive and time-consuming. Second, due to the overall immaturity of quantum technologies, many advanced quantum network protocols and schemes, such as all-photonic entanglement-based repeater protocols [16], remain in the conceptual stage and cannot be realized in the current quantum network testbeds. Third, existing quantum network testbeds have only a few nodes. Thus, it is impossible to conduct scalability research in such environments.

Quantum network modeling and simulation offers a powerful and cost-effective alternative to study quantum networks without requiring physical networks. It can help in understanding the relative performance and resource requirements of different types of quantum networks, tradeoffs of alternative quantum network architectures, optimizing quantum hardware, and developing a robust control plane. NetSquid is a software tool for the modeling and simulation of scalable quantum networks developed at QuTech [17]. The Lawrence Berkeley National Laboratory (LBNL) quantum network research team, along with Economou's research group, is developing a quantum repeater toolkit based on NetSquid to study advanced quantum repeaters and networks. In this paper, we present our initial research findings on modeling and simulation

QuNet '25, Coimbra, Portugal

ACM ISBN 979-8-4007-2097-0/25/09
https://doi.org/10.1145/3749096.3750024

Charu Jain*, Chuen Hei Chan*+, Ezra Kissel*, Wenji Wu*, Inder Monga*
*Lawrence Berkeley National Laboratory, +Virginia Tech, USA

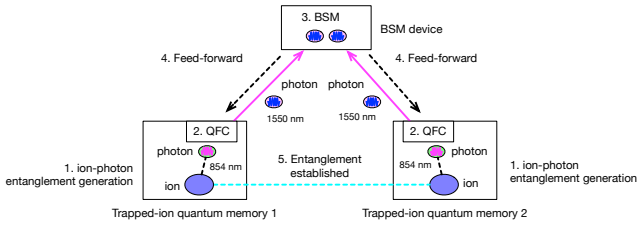

Figure 1: HEG between two remote $^{40}Ca^{+}$ ions.

of trapped ion quantum repeaters and networks. Our analysis and simulation work is based on trapped $^{40}Ca^{+}$ ions [6, 9, 15], which represents the state-of-the-art in this area. We study the performance and resource requirements of trapped-ion quantum networks. The performance metrics include end-to-end entanglement generation rate and fidelity of the network.

The contributions of our work are the following. First, we employ a rigorous and holistic approach to the simulation of trapped ion quantum networks. A unique advantage of our approach is that the consideration of the analog processes and dynamics of the QRs will allow us to accurately simulate real-world trapped-ion QRs and networks. Second, our study and analysis identify important parameters that have impact on quantum network performance metrics including entanglement generation rate and fidelity. Such results can guide the research and development of trapped-ion QR technologies and the design and construction of practical trapped ion quantum networks.

The rest of the paper is organized as follow. Section 2 presents trapped-ion QRs and networks. Section 3 discusses our design and implementation of trapped-ion QRs and networks using NetSquid. Section 4 presents the simulation results and discussion. Section 5 concludes the paper.

2 Trapped-ion QRs and networks

In this section, we present how a trapped ion network works. We first introduce the major quantum components that constitute a trapped-ion quantum network: (a) *Quantum end nodes (Q-nodes)* are much like classic end nodes, representing the communication parties in a quantum network. (b) *Quantum Repeaters (QRs)* can extend a quantum network to a larger distance by mitigating loss and correcting errors. (c) *Bell-State-Measurement nodes (BSM-nodes)* can perform BSM and local Pauli operations for incoming photons. And (d) *Quantum and classical channels.* Q-nodes, QRs, and BSM-nodes are connected to each other through optical fibers. Dedicated wavelengths of these fibers are used as quantum and classical channels to transmit information between them.

2.1 Heralded entanglement generation

Because entanglement generation is a probabilistic process, heralded entanglement generation (HEG) allows for confirmation that an entangled state has been successfully created so that it can be used for further operations. A heralded ion-ion entanglement establishing process between two $^{40}Ca^{+}$ trapped-ion systems is illustrated in Fig. 1. This process relies on the synchronous preparation of entanglement between the electronic degree-of-freedom of a trapped ion and the polarization of a photon within each trapped-ion system. Each cycle starts with ion state initialization, followed by a Raman pulse that triggers an emission of a 854 nm-photon into the cavity mode. After quantum frequency conversion (QFC), the resulting photon in the telecom-band, entangled with the ion, is transmitted towards a BSM device in an attempt to create ion-ion entanglement via a projective measurement in the Bell basis of the polarization states. If no Bell state has been detected, each system continues the entanglement generation attempts. If a two-fold coincidence has been detected at the BSM device, it signals projection into a Bell state ion-ion entanglement and each node is instructed to stop to preserve entanglement. This ion-ion entanglement is stored as a resource for future use.

2.2 Entanglement swapping

Entanglement swapping concatenates segment entanglements of short distance into end-to-end entanglement of long distance. Based on Lanyon's group recent experimental realization of a quantum repeater based on trapped $^{40}Ca^{+}$ ions [9], we present how a quantum repeater performs such a function. As illustrated in Fig. 2, an elementary quantum network consists of two Q-nodes, two BSM-nodes, and a QR. Q-node 1 and 2 each has one $^{40}Ca^{+}$ ion, a A' and B', respectively. The QR is based on two $^{40}Ca^{+}$ ions, A and B, which are trapped in a linear Paul trap. To achieve greater emission efficiency, the trap is coupled to a high-finesse optical cavity. Because both ion A and B are trapped in a linear Paul trap that is coupled to a cavity, HEG operations that involve ion A and B must be performed in sequence to avoid simultaneous 854 nm-photon emissions into the cavity.

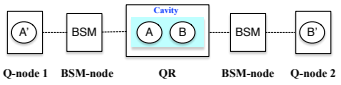

Figure 2: A quantum network based on trapped $^{40}Ca^{+}$ ions.

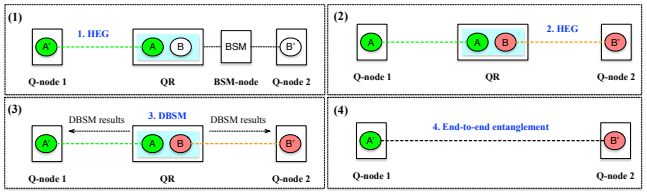

Figure 3: Entanglement swapping and end-to-end entanglement generation.

As illustrated in Fig. 3, the end-to-end entanglement generation process between Q-node 1 and 2 works as follows. (1) HEG is performed between ion A' of Q-node 1 and ion A of QR. A heralding signal confirms segment entanglement A' ↔ A has been successfully generated. (2) HEG is performed between ion B of QR and ion B' of Q-node 2. Similarly, a heralding signal confirms segment entanglement B ↔ B' has been successfully created. (3) Deterministic Bell State Measurement (DBSM) is performed between ion A and B at QR, with measurement outcomes sent to Q-node 1 and 2, respectively. The DBSM is performed in two steps. First, a laser-driven two-qubit Mølmer-Sørensen (MS) logic gate is applied on A and B. Second, the logical state of ion qubit A and B is measured via

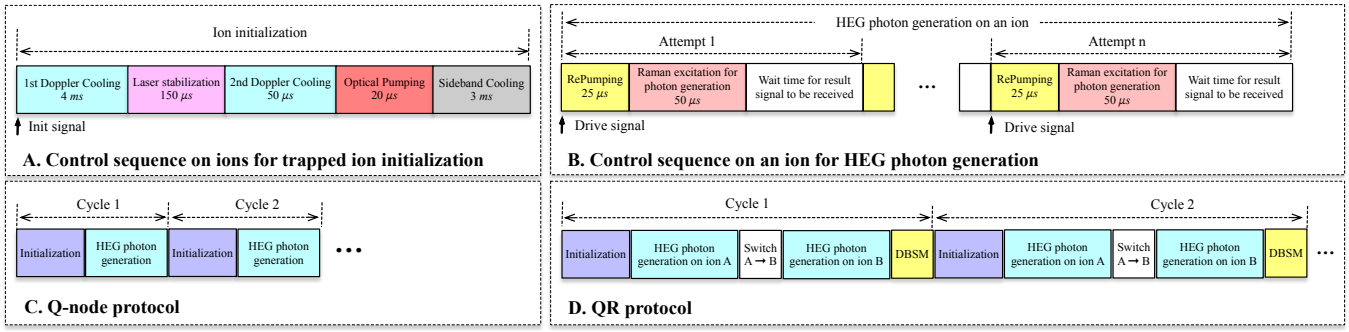

Figure 4: Control sequences and protocols for Q-node and QR models.

fluorescence detection. (4) Based on BSM outcomes, corresponding Pauli operations are applied on ion A' of Q-node 1 and ion B' of Q-node 2, respectively. End-to-end entanglement A' ↔ B' is successfully established.

3 Design and Modeling using NetSquid

We developed building block node models that correspond to the major entities in a trapped ion quantum network (i.e., Q-node, QR, and BSM-node), and a control node that supports logically centralized control. The details are described below.

3.1 BSM-node model

As discussed in Section 2.1, a trapped ion is driven by a sequence of laser pulses to generate photons. Therefore, we can vary a Q-node's, or a QR's, photon generation time by properly controlling its drive pulses. As such, we implemented a clock-assisted scheme to realize heralded entanglement generation. In our design, each BSM-node model includes a local clock and a BSM unit that connects to two neighboring nodes. A neighboring node can be either a Q-node or a QR. In operation, a BSM-node generates and transmits clock signals to each of its neighboring nodes through a classical channel to trigger photon generation. For BSM, because the photon's time-of-flight from the two neighboring nodes to the BSM-node are different, the BSM-node can control its neighboring nodes' photon generation time by adjusting the relative timing between clock signals to each neighboring node accordingly so that the generated photons arrive at the BSM-node simultaneously.

3.2 Q-node and QR models

Our Q-node and QR models are based on the recent experimental realization of light-matter interfaces [15] and QRs that are based on $^{40}Ca^{+}$ [9]. Each Q-node model has a single ion in a trap, and each QR model simulates two trapped ions, termed A and B, which are coupled to a cavity. We developed models to simulate the underlying physical processes that govern trapped-ion dynamics, which include: (a) *Ion initialization* that initializes ions for HEG and (b) *HEG photon generation* that prepares and excites an ion to generate photons for HEG. A photon generation process consists of up to n attempts. Each attempt is triggered by *a clock signal* from a BSM-node. The process terminates when any attempt succeeds; otherwise up to n attempts will be made until the process exits with failure. Based on these building blocks, a Q-node protocol and a QR protocol were developed for entanglement generation (see Fig. 4). Both protocols runs continuously in cycles. For the Q-node protocol, each cycle consists of two phases: *ion initialization* and *photon generation*. For the QR protocol, each cycle consists of four phases: *ion A and B initialization*, *HEG photon generation on ion A*, *switch A → B*, *HEG photon generation on ion B*, and *DBSM*.

3.3 A two-step approach for parallel HEGs

As discussed in Section 2.2, when both ion A and B are trapped in a linear trap that is coupled to a cavity, HEG operations that involve ion A and B must be performed sequentially to avoid simultaneous photon emission into the cavity. Therefore, to satisfy such a constraint, parallel HEG operations are not allowed in the neighboring segments along a QR chain. While linear, hop-by-hop HEG may be an obvious first choice, a more efficient protocol is to conduct parallel HEG operations on alternating segments to avoid resource conflicts. Using centralized resource scheduling with knowledge of the repeater chain resources, the overall HEG operations can be completed in a maximum of two phases, regardless of the number of QRs involved in the chain.

3.4 Logically centralized control

We designed and implemented a logically centralized control for a trapped ion quantum network. A control-node controls and orchestrates the underlying quantum network devices. Such a design facilitates end-to-end entanglement generation in a trapped ion quantum network. As illustrated in Fig. 5, to start entanglement generation between two Q-nodes in a network, the control-node first performs routing (Step 1) to choose a path between the two Q-nodes, next activates the two-step approach to conduct HEGs in the path (Step 2 and 3). As soon as HEGs are completed, DBSMs are performed in QRs (Step 4). DBSM outcomes are transmitted from each BSM-node to the control-node through classical channels. Upon receiving the outcomes of every BSM-nodes, the control-node will determine whether the entanglement generation is successful and require Pauli frame adjustment. These would then be sent to both end Q-nodes through classical channels (Step 5). In the successful case, each end Q-node would perform the suitable Pauli frame adjustment to the corresponding matter qubit.

Charu Jain*, Chuen Hei Chan*+, Ezra Kissel*, Wenji Wu*, Inder Monga*
*Lawrence Berkeley National Laboratory, +Virginia Tech, USA

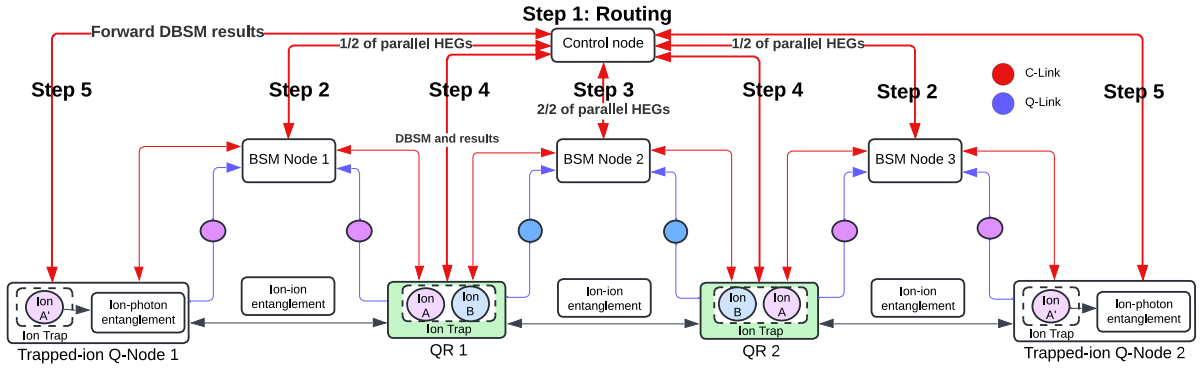

Figure 5: Logically centralized control.

4 Simulation Results

In this section, we present our simulation of trapped-ion quantum networks using NetSquid. We simulated a QR chain of the form $Q_1 \leftrightarrow BSM_1 \leftrightarrow QR_1 \ldots QR_n \leftrightarrow BSM_{n+1} \leftrightarrow Q_n$. The nodes in the chain are evenly spaced. The chain distance between Q-nodes Q_1 and Q_n, as well as the number of QRs (n) in the chain, are varied across different simulations. In our simulation, the matter qubits and light-matter interfaces within each trapped ion QR are simulated using parameters from the state-of-the-art experiments [9, 15, 18–20]. Photon loss is modeled at each quantum channel, with a signal attenuation rate of $\alpha = 0.2dB/km$. This gives the overall transmission probability $\sim 10^{-\frac{\alpha}{L}}$, where L is the length of the quantum channel. Unless otherwise noted, the parameter choices in our simulations are listed in Tables 1.

Parameters	Value
Single qubit gate fidelity	$\geq 99.995\%$
Two qubit gate fidelity	99.9%
Coherence time	$60ms$
Ion-photon entanglement fidelity	96%
QFC efficiency	0.3
Detector efficiency	0.75
Ion-trap collection efficiency	0.69
Single qubit gate duration	$5\mu s$
Mølmer-Sørensen gate duration	$107\mu s$
Fiber loss	$0.2dB/km$

Table 1: Simulation parameters

Through simulation, we study the performance and resource requirements of trapped-ion quantum networks. The performance metrics include entanglement generation rate and fidelity between the end nodes of the network. The rate is determined by dividing the number of successful events by the total time taken for all trials, giving successful entanglement attempts per second. The fidelity is calculated as $F = \langle \Psi^+ | \rho | \Psi^+ \rangle \in [0, 1]$. Here, $|\Psi^+\rangle$ is a reference Bell state, and ρ is the density matrix of an entangled pair. It is averaged over multiple trials and the standard error of the mean (SEM) is used to quantify the uncertainty in this average fidelity, calculated as the standard deviation of fidelity values divided by the square root of the number of successful trials.

We carefully verified and validated the simulation results. The simulation results of the trapped ion QR chains were verified and validated using experiment data [9, 15].

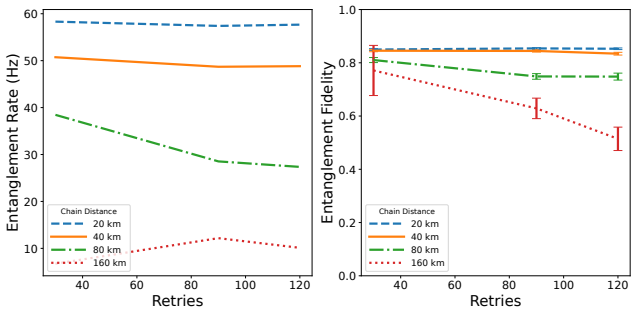

Figure 6: Entanglement generation rate and fidelity with the HEG retry limit and the chain distance varied. The number of QRs is set to 1.

4.1 HEG retry limit

In our design, HEG is implemented with retries, up to a retry limit (see Section 2.1). As illustrated in Fig. 6, at a chain distance of $20km$ or $40km$, HEG retry limit does not have an impact on the performance; at $80km$ or $160km$, fidelity significantly decreases as the retry limit is increased. This is because in a larger quantum network, transmitting photons and passing messages takes more time, and increasing the HEG retry limit will significantly increase the overall entanglement generation process overheads. As a result, decoherence will lead to degraded fidelity. Fig. 6 also shows that HEG retry limit is a difficult parameter to select for a larger network (e.g. with a chain distance of $160km$). A "just right" parameter, not too big or not too small, should be chosen to achieve an appropriate rate. A trade-off between rate and fidelity should be considered. In our simulations, the HEG retry limit is set to 90. Fig. 7 shows the Cumulative Distribution Functions (CDFs) of the HEG retries of successful entanglement generation in a chain with the distance varied and the number of QRs set to 1. The statistical method identifies a 90% cumulative success, shown as vertical lines, enabling efficient retry determination.

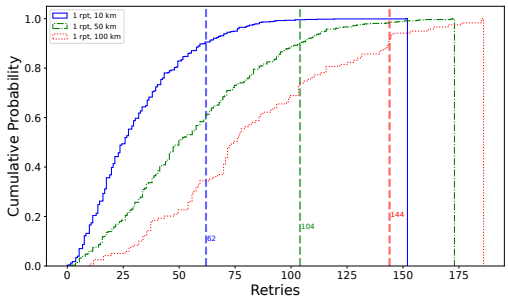

Figure 7: CDF plots for the HEG retries of successful entanglement generation with the chain distance varied and the number of QRs set to 1. A lower bound fidelity threshold of 0.7 is set.

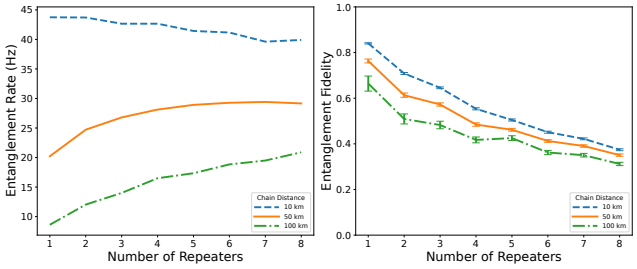

Figure 8: Entanglement generation rate and fidelity with the chain distance and the number of QRs varied.

4.2 The chain distance and the number of quantum repeaters

We study the impact on entanglement generation rate and fidelity when the chain distance and the number of QRs of a trapped ion QR chain are varied. As illustrated in Fig. 8, at a chain distance of $10km$, entanglement generation rate decreases as the number of QRs in the chain is increased; at a chain distance of $50km$ or $100km$, entanglement generation rate increases as the number of QRs is increased. The major function of QRs is to divide the end-to-end long distance of quantum links into shorter intermediate segments connected by QRs, in which photon loss from fiber attenuation can be corrected. Although adding repeaters in a chain helps to reduce photon loss in quantum links, it also introduces overheads that can be attributed to the collection efficiency of photon, quantum frequency conversion efficiency, and photon detector efficiency, etc. The entanglement rate will decrease when the benefits of adding repeaters in a chain are less than the incurred overheads. Fig. 8 also shows that the fidelity decreases with the number of repeaters, regardless of the chain distance. This is because QRs are mainly designed to mitigate against photon loss in order to improve entanglement generation rate. However, the functioning of QRs necessarily introduces noise, leading to infidelity. The effect of infidelity is cumulative, which increases with the number of repeaters. To improve entanglement fidelity, advanced mechanisms such as quantum error correction or quantum distillation are required.

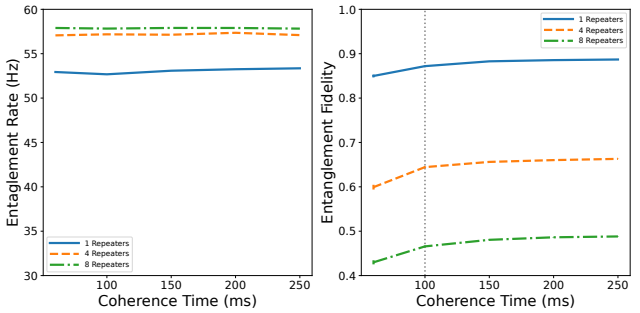

Figure 9: Entanglement generation rate and fidelity with the $^{40}Ca^{+}$ qubit coherence time varied. The chain distance is set to $50km$. Note: SEM is small in the figure.

4.3 $^{40}Ca^{+}$ coherence time

The state-of-art $^{40}Ca^{+}$ qubit under working conditions has a coherence time of $60ms$ [9]. In our simulations, we varied the emitter coherence time from $60ms$ to $250ms$ to study the impact of emitter coherence time on the entanglement generation rate and fidelity. As shown in Fig. 9, fidelity improves when the coherence time is increased from $60ms$ to $100ms$ while there are slight fidelity improvement with the coherence time further increased, regardless of the number of repeaters simulated. This is because entanglement fidelity is calculated at the time of successful entanglement establishment while most entanglement generation time is less than $100ms$ at a chain distance of $50km$. But longer coherence time will definitely help entanglement storage in ion qubits for future use. Fig. 9 also shows varying coherence time does not affect the entanglement rate.

4.4 QFC efficiency

Researchers demonstrated polarization-preserving frequency conversion of single-photon-level light at $854nm$ to the $1550nm$ telecom C band, with a total photon in/fiber-coupled photon out efficiency of $\sim$ 30% [19]. In our simulations, we varied QFC efficiency from 30% to 90% to study the impact of QFC efficiency on the entanglement generation rate and fidelity. As shown in Fig. 10, increasing QFC efficiency significantly improves entanglement generation rate. However, varying coherence time does not affect the entanglement rate.

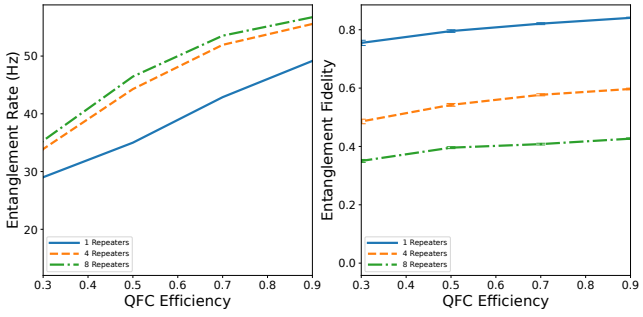

Figure 10: Entanglement generation rate and fidelity with the QFC efficiency varied. The chain distance is set to $50km$.

Table 2: Simulation results on representative ESnet dark fiber links using current and future ion-trap parameters.

Path	Dist.	PathQRs	Current Rate	Current Fidelity	Future Rate	Future Fidelity
CHIC–FNALGCC	55 km	2	22.11 Hz	0.56	52.28 Hz	0.95
LBNL50–SUNN	84 km	6	24.20 Hz	0.37	50.76 Hz	0.89
CHAT–NASH	180 km	3	2.04 Hz	0.43	24.30 Hz	0.90

4.5 Discussion and future work

Using state-of-art parameters, our simulations show entanglement rates and fidelity for a trapped-ion QR platform up to roughly 200km end-to-end distance. We might then ask – *to what extent are trapped-ion quantum networks deployable on existing, real-world fiber infrastructure*? We investigate ESnet's U.S. deployed dark fiber network [1] (Fig. 11) as one such scenario, and identify 30 points-of-presence (PoPs) in the network where trapped-ion QRs might be deployed. There are 429 identified shortest paths among those 30 PoPs, each with varying number of classical amplification sites spaced ~50km on average. Each of these sites may be candidates for an ion trap QR deployment along the path.

Among those 429 paths, we extracted 25 (~6%) with 8 or fewer intermediate hubs and end-to-end distances ranging from 10 km to 200 km. These paths are analogous to the number of repeaters and the total chain distance, respectively, in our quantum network simulations. We simulated quantum repeater performance on selected ESnet dark fiber links to evaluate entanglement generation rate and fidelity under both current (Table 1) and future ion-trap conditions. Table 2 reports results for three representative links, comparing the maximum possible path-defined, repeater placement (PathQRs). Simulations incorporating major future hardware improvements (QFC efficiency of 0.9, Mølmer–Sørensen (MS) gate fidelity of 0.99, 200 ms coherence time, and fiber loss of 0.1 dB/km) show significant increases in both rate and fidelity. We clearly see the limited reach of current trapped ion platforms in providing usable end-to-end entanglement fidelity for distributed quantum computing applications at distance. With future advancements in underlying quantum technologies, and with the introduction of advanced purification schemes and quantum error correction mechanisms, we expect QR chains to become practical for a wider range of real-world fiber networks.

[1] https://www.es.net/engineering-services/the-network/

Figure 11: ESnet dark fiber topology. Each node represents either a POP or classical amplification station.

In this paper, we study entanglement generation between a single pair of remote $^{40}Ca^{+}$ ions by simulating a QR chain. While entanglement rate benefits from larger number of repeaters, an interesting finding of this work is that the fidelity decreases with the increase of the number of QRs in the chain, regardless of the chain distance. The QR chain studied in this paper has the minimum resource requirements because each Q-node model features a single $^{40}Ca^{+}$ ion and each QR model simulates two $^{40}Ca^{+}$ ions. However, this QR chain has inherently limited rate and fidelity. Multiplexed entanglement generation is a promising technique in quantum networking that utilizes multiple qubits within a single node to create and distribute entanglement more efficiently. With simultaneous creation of multiple entangled states, multiple entangled states with lower fidelity can be purified into a smaller number of entangled states with higher fidelity. We leave multiplexed entanglement generation and purification to future work.

5 Conclusion

In this paper, we employ a rigorous and holistic approach to the simulation of trapped ion quantum networks using NetSquid. A unique advantage of our approach is that the consideration of the analog processes and dynamics of the quantum repeaters will allow us to accurately simulate real-world trapped ion quantum repeaters and networks. The simulation code of this work can be found at https://github.com/qlbnl/qnpack.

6 Acknowledgements

This research is supported by the Quantum Internet to Accelerate Scientific Discovery ASCR Research Program funded through Berkeley Lab FWP FP00013429, and by Berkeley Lab LDRD 25-153. The U.S. Government retains, and the publisher, by accepting the article for publication, acknowledges, that the U.S. Government retains a non-exclusive, paid-up, irrevocable, world-wide license to publish or reproduce the published form of this manuscript, or allow others to do so, for U.S. Government purposes. See the content disclaimer below.[2]

References

[1] Youpeng Zhong, Hung-Shen Chang, Audrey Bienfait, Étienne Dumur, Ming-Han Chou, Christopher R Conner, Joel Grebel, Rhys G Povey, Haoxiong Yan, David I Schuster, et al. Deterministic multi-qubit entanglement in a quantum network. *Nature*, 590(7847):571–575, 2021.

[2] Peter C Humphreys, Norbert Kalb, Jaco PJ Morits, Raymond N Schouten, Raymond FL Vermeulen, Daniel J Twitchen, Matthew Markham, and Ronald Hanson. Deterministic delivery of remote entanglement on a quantum network. *Nature*, 558(7709):268–273, 2018.

[3] SLN Hermans, Matteo Pompili, HKC Beukers, Simon Baier, Johannes Borregaard, and Ronald Hanson. Qubit teleportation between non-neighbouring nodes in a quantum network. *Nature*, 605(7911):663–668, 2022.

[4] Severin Daiss, Stefan Langenfeld, Stephan Welte, Emanuele Distante, Philip Thomas, Lukas Hartung, Olivier Morin, and Gerhard Rempe. A quantum-logic gate between distant quantum-network modules. *Science*, 371(6529):614–617, 2021.

[5] Manuel Brekenfeld, Dominik Niemietz, Joseph Dale Christesen, and Gerhard Rempe. A quantum network node with crossed optical fibre cavities. *Nature Physics*, 16(6):647–651, 2020.

[6] V Krutyanskiy, M Galli, V Krcmarsky, S Baier, DA Fioretto, Y Pu, A Mazloom, P Sekatski, M Canteri, M Teller, et al. Entanglement of trapped-ion qubits separated by 230 meters. *Physical Review Letters*, 130(5):050803, 2023.

[7] LJ Stephenson, DP Nadlinger, BC Nichol, S An, P Drmota, TG Ballance, K Thirumalai, JF Goodwin, DM Lucas, and CJ Ballance. High-rate, high-fidelity entanglement of qubits across an elementary quantum network. *Physical review letters*, 124(11):110501, 2020.

[8] Matthias Bock, Pascal Eich, Stephan Kucera, Matthias Kreis, Andreas Lenhard, Christoph Becher, and Jürgen Eschner. High-fidelity entanglement between a trapped ion and a telecom photon via quantum frequency conversion. *Nature communications*, 9(1):1998, 2018.

[9] Victor Krutyanskiy, Marco Canteri, Martin Meraner, James Bate, Vojtech Krcmarsky, Josef Schupp, Nicolas Sangouard, and Ben P Lanyon. Telecom-wavelength quantum repeater node based on a trapped-ion processor. *Physical Review Letters*, 130(21):213601, 2023.

[10] John P Gaebler, Ting Rei Tan, Yiheng Lin, Y Wan, Ryan Bowler, Adam C Keith, Scott Glancy, Kevin Coakley, Emanuel Knill, Dietrich Leibfried, et al. High-fidelity universal gate set for be 9+ ion qubits. *Physical review letters*, 117(6):060505, 2016.

[11] CJ Ballance, TP Harty, NM Linke, MA Sepiol, and DM Lucas. High-fidelity quantum logic gates using trapped-ion hyperfine qubits. *Physical review letters*, 117(6):060504, 2016.

[12] TP Harty, DTC Allcock, C J Ballance, L Guidoni, HA Janacek, NM Linke, DN Stacey, and DM Lucas. High-fidelity preparation, gates, memory, and readout of a trapped-ion quantum bit. *Physical review letters*, 113(22):220501, 2014.

[13] Anna Keselman, Yinnon Glickman, Nitzan Akerman, Shlomi Kotler, and Roee Ozeri. High-fidelity state detection and tomography of a single-ion zeeman qubit. *New Journal of Physics*, 13(7):073027, 2011.

[14] M Meraner, A Mazloom, V Krutyanskiy, V Krcmarsky, J Schupp, DA Fioretto, P Sekatski, TE Northup, N Sangouard, and BP Lanyon. Indistinguishable photons from a trapped-ion quantum network node. *Physical Review A*, 102(5):052614, 2020.

[15] J Schupp, V Krcmarsky, V Krutyanskiy, M Meraner, TE Northup, and BP Lanyon. Interface between trapped-ion qubits and traveling photons with close-to-optimal efficiency. *PRX quantum*, 2(2):020331, 2021.

[16] Koji Azuma, Kiyoshi Tamaki, and Hoi-Kwong Lo. All-photonic quantum repeaters. *Nature communications*, 6(1):1–7, 2015.

[17] Tim Coopmans, Robert Knegjens, Axel Dahlberg, David Maier, Loek Nijsten, Julio de Oliveira Filho, Martijn Papendrecht, Julian Rabbie, Filip Rozpedek, Matthew Skrzypczyk, et al. Netsquid, a network simulator for quantum information using discrete events. *Communications Physics*, 4(1):164, 2021.

[18] Kenneth R Brown, John Chiaverini, Jeremy M Sage, and Hartmut Häffner. Materials challenges for trapped-ion quantum computers. *Nature Reviews Materials*, 6(10):892–905, 2021.

[19] V Krutyanskiy, M Meraner, J Schupp, and BP Lanyon. Polarisation-preserving photon frequency conversion from a trapped-ion-compatible wavelength to the telecom c-band. *Applied Physics B*, 123(9):228, 2017.

[20] U. G. Poschinger, G. Huber, F. Ziesel, M. Deiss, M. Hettrich, S. A. Schulz, K. Singer, F. Schmidt-Kaler, G. Poulsen, M. Drewsen, and R. J. Hendricks. Coherent manipulation of a ca spin qubit in a micro ion trap. *arXiv preprint arXiv:0902.2826*, 2009.